

A PRACTICAL BIODYNAMIC FEEDTHROUGH MODEL FOR HELICOPTERS

Joost Venrooij^{1,2}, Marilena D. Pavel², Max Mulder²,
Frans C. T. van der Helm², Heinrich H. Bühlhoff^{1,3}

¹*Max Planck Institute for Biological Cybernetics, Tübingen, Germany
(joost.venrooij,heinrich.buelthoff)tuebingen.mpg.de*

²*Delft University of Technology, Delft, The Netherlands
(j.venrooij,m.d.pavel,m.mulder,f.c.t.vanderhelm)tudelft.nl*

³*Korea University, Seoul, Korea*

Abstract

Biodynamic feedthrough (BDFT) occurs when vehicle vibrations and accelerations feed through the pilot's body and cause involuntary motion of limbs, resulting in involuntary control inputs. BDFT can severely reduce ride comfort, control accuracy and, above all, safety during the operation of rotorcraft. Furthermore, BDFT can cause and sustain Rotorcraft-Pilot Couplings (RPCs). Despite many studies conducted in past decades – both within and outside of the rotorcraft community – BDFT is still a poorly understood phenomenon. The complexities involved in BDFT have kept researchers and manufacturers in the rotorcraft domain from developing robust ways of dealing with its effects. A practical BDFT pilot model, describing the amount of involuntary control inputs as a function of accelerations, could pave the way to account for adverse BDFT effects. In the current paper, such a model is proposed. Its structure is based on the model proposed by Mayo [1], its accuracy and usability are improved by incorporating insights from recently obtained experimental data. An evaluation of the model performance shows that the model describes the measured data well and that it provides a considerable improvement to the original Mayo model. Furthermore, the results indicate that the neuromuscular dynamics have an important influence on the BDFT model parameters.

1. INTRODUCTION

Biodynamic feedthrough (BDFT) occurs when vehicle vibrations and accelerations feed through the pilot's body and cause involuntary motion of limbs. Especially the involuntary motions of torso, arms and hands can degrade manual control performance as they may lead to involuntary control inputs. BDFT can severely reduce ride comfort, control accuracy and, above all, safety during the operation of a large range of different vehicles, e.g., hydraulic excavators [2], aircraft when flying through atmospheric turbulence [3] or during roll-ratcheting [4], and electrically powered wheelchairs [5]. Aircraft handling qualities are known to degrade due to BDFT effects [6, 7], and also for rotorcraft the pilot control performance can suffer from the effects of BDFT [8, 1, 9].

The occurrence of BDFT in helicopters has been under investigation for several decades. One of the earlier studies was done by Gabel and Wilson (1968), where vertical bounce (also known as collective bounce) was investigated [8]. Vertical bounce is

a divergent, vertical helicopter oscillation caused by an interaction between the vertical motion of the helicopter and the pilot's body, where involuntary motions of the pilot's arm are coupled to the collective pitch stick. Another example of a study investigating BDFT in helicopters was performed by Mayo in 1989 [1]. Here, the effects of BDFT in the helicopter collective control loop were measured, modeled, and simulated. Other, more recent studies regarding BDFT in helicopters have been conducted in the context of the GARTEUR HC-AG16 project (e.g., [10]) and the ARISTOTEL project (e.g., [11, 12, 13, 14]). In these projects, so-called Rotorcraft-Pilot Couplings (RPCs) were/are investigated. RPCs (also, until the mid 1990s, known under the name of Pilot Induced/Assisted Oscillations (PIOs/PAOs)) are oscillations or divergent responses of a vehicle originating from adverse pilot-vehicle couplings. Biodynamic feedthrough can cause and sustain such events. Recently, RPCs have received more attention in the design, testing and operation of rotorcraft. An important reason for this is that with the rapid advances in the field of flight-control-systems (FCS) rotorcraft seem more sensitive to the appearance of RPC events

[15, 16], stressing the need to better understand how BDFT may interfere with control performance in order to predict, evaluate and alleviate its effects on RPCs. Despite many studies conducted in past decades – both within and outside of the rotorcraft community – BDFT is still a poorly understood phenomenon. Many factors are known to influence BDFT dynamics [17] but undoubtedly the most complex source of variation in BDFT dynamics is the human operator. Not only *between-subject variability* has shown to be of importance – i.e., differences in body characteristics such as weight and size [1, 18] – but also *within-subject variability* is of great importance – i.e., time-varying factors such as workload [1] and task interpretation [19]. Modeling or accounting for both sources of variability has proven to be a challenging task. In literature, between-subject variability is often reported but only occasionally dealt with. The study by Mayo is an exception, as it particularly investigates one source of between-subject variability, namely body type [1]. More details regarding this study are provided in the next section.

Studies examining the topic of within-subject BDFT variability seem to be even more rare. Once more, in many publications the possibility that BDFT dynamics may vary over time, as results of ‘muscle activity’ or ‘control strategy’, is mentioned, but generally not investigated in any detail. Recently, a method was developed to measure BDFT and neuromuscular admittance (a measure for limb dynamics) simultaneously [20]. Neuromuscular admittance, or simply admittance, is a measure for describing the limb dynamics of the subject’s body and represents a dynamical relationship between force input and position output. The admittance contains the effect of both static features (e.g., limb weight) and time-varying features (e.g., muscle co-contraction). This makes neuromuscular admittance an insightful instrument in understanding BDFT. The results showed a strong dependency of BDFT dynamics on admittance, which itself is depending on the control task performed or the control strategy selected by the pilot [21]. With the results of this method it was also shown that effective cancellation of BDFT requires a subject- and task-dependent approach, i.e., accounting for both between- and within-subject variability [22]. Simulations suggest that not accounting for either of them leads to suboptimal control actions or even a complete failure of the cancellation.

The complexities of BDFT, and especially the present limited understanding of this phenomenon, have kept researchers and manufacturers in the rotorcraft domain from developing robust ways of dealing with BDFT (and RPCs). One of the possible applications of this knowledge could be, for example, the determination of the susceptibility of a particular vehicle design or control device layout to RPCs in an early stage

in the design process. To allow for such analyses, a BDFT model, describing the amount of involuntary control inputs as a function of accelerations, would be the appropriate tool.

Elaborate BDFT models have been developed (e.g., [23]), but these are rarely used in practice as they are too unwieldy to be implemented in a sensible way in the design process. Instead, more basic and therefore more practical models, such as proposed by Mayo [1], are used (e.g. in [10, 24, 25, 26, 13]). The simplicity and direct applicability of Mayo’s pilot model seems to be an important trait. The model contains only four parameters, for which values were provided for the different body types. However, the drawbacks of a ‘simple’ model are apparent too: such a model can never account for the complexities encountered in reality and is bound to be inaccurate when circumstances deviate from the intended conditions. The challenge of balancing a model’s accuracy with the model’s usability is a difficult one, but in general it can be said that many helicopter manufacturers and researchers would benefit from a BDFT pilot model, dedicated to rotorcraft, which is directly applicable and easy to use.

In the current paper, a practical BDFT pilot model is proposed for rotorcraft. Its structure is based on the model proposed by Mayo, its accuracy and usability are improved by incorporating insights from recently obtained experimental data. The model is independent from vehicle dynamics and can thus be used in simulation with a large range of helicopter dynamic models to investigate closed-loop interactions between pilot and vehicle. Between-subject variability is accounted for by providing model parameters for different body types. Within-subject variability – the most significant extension of Mayo’s original model – is accounted for by providing model parameters as a function of the pilot’s neuromuscular adaptation to different tasks.

2. MAYO’S BDFT PILOT MODEL

In the following, the details of the model as proposed by Mayo in Ref. [1] are discussed. This model will be referred to as the Mayo (pilot) model.

2.1. Experiment description

In Mayo’s experiment, the pilot’s collective stick motion was recorded while the pilot was being perturbed using vertical, sinusoidal acceleration disturbances of discrete single frequencies, ranging from 1 to 5 Hz , in 0.5 Hz increments. The duration of each disturbance signal was approximately 3 minutes. The simulator cockpit was set up with the conventional helicopter seat, and controls, i.e., cyclic, collective and

pedals. The control dynamics were set to “typical” values (no further details provided in the original publication), with the exception of the deadband region of each inceptor, which was removed to eliminate nonlinearities. No outside visuals were provided. The measurement devices were two three-axes accelerometers, which were mounted on the collective grip and at the center of the pilot’s seat, recording at 30 Hz. To maintain natural grip during the BDFT measurement, the subjects were instructed to perform a low-frequency tracking task. The task was performed using both the longitudinal cyclic (fore-aft) and the collective stick in order to simultaneously track two low-frequency signals, indicated by two needles in the cockpit. Each inceptor controlled a needle which was moving sinusoidally around a trim point. The objective was to keep each pointer at the center trim position. The experiment was performed in an ‘open-loop’ fashion, meaning that the control input provided by the pilot did not influence the acceleration of the motion platform. The tracking signals were of “sufficiently low frequency” to be spectrally separable from the BDFT measurement.

A total of six participants, with different body types and piloting experience, participated in the experiment. To generalize the differences in anthropometric types the results were averaged for “three distinctly mesomorphic” (athletic bone structure and muscle build) subjects and for “three distinctly ectomorphic” (slim bone structure and muscle build) subjects. The average height was 175.3 cm for the ectomorphic subjects, and 185.4 cm for mesomorphic subjects. The average weight was 69.0 kg for the ectomorphic subjects, and 89.8 kg for mesomorphic subjects. Meso- and ectomorph are two of the three somatotypes as proposed by Sheldon et al. [27]. The third somatotype is endomorphic (not measured in [1]) and can be characterized as having a large bone structure and muscle build.

2.2. The Mayo pilot model

To describe the experimental results, Mayo proposed the following transfer function pilot model, which describes the absolute acceleration of the hand holding the collective as a function of the seat’s vertical acceleration [1]:

$$(1) \quad H_{mayo,abs}(s) = \frac{a_1 s + a_2}{s^2 + b_1 s + b_2},$$

where s represents the Laplace operator. The values of the four parameters a_1 , a_2 , b_1 and b_2 were found by fitting the transfer function on the data obtained for the two somatotypes. Slight differences between the BDFT dynamics for the two somatotypical groups were reported. The resulting models for ectomorphic

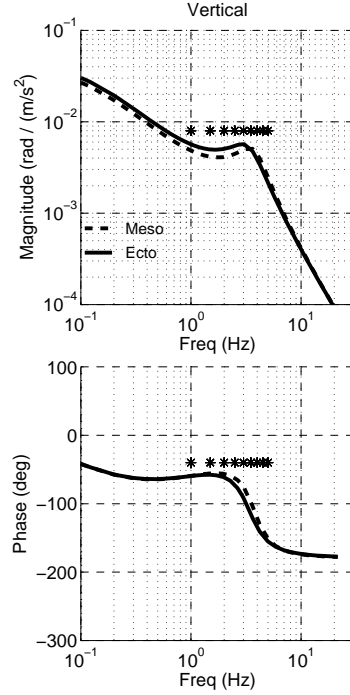


Figure 1: *The adapted Mayo model (Eq. 4) for ecto- and mesomorphic subjects. The asterisks indicate the frequencies where acceleration disturbances were applied in Ref. [1].*

and mesomorphic subjects were:

$$(2) \quad H_{mayo,abs}^{ecto}(s) = \frac{5.19s + 452.3}{s^2 + 13.7s + 452.3}$$

and

$$(3) \quad H_{mayo,abs}^{meso}(s) = \frac{4.02s + 555.4}{s^2 + 13.31s + 555.4}$$

2.3. Adapting the Mayo model

The transfer functions in Eqs. 1-3 describe the absolute acceleration, in m/s^2 , of the hand holding the collective as a function of the seat’s vertical acceleration, in m/s^2 . In order to compare this model with the BDFT results obtained in this study, it needs to be adapted to obtain relative control device deflection, in rad , as a function of the seat’s vertical acceleration, in m/s^2 . This can be done, as described in [12], by adding a two pseudo-integrators ($1/(s + c)$), converting acceleration to position, and by dividing by the length of the inceptor L , in m , approximating deflection in rad . To obtain the relative deflection one needs to subtract the absolute acceleration of seat from the absolute acceleration of the hand, resulting in $H_{mayo,abs}(s) - 1$. The relative deflection of the control device as a function of the acceleration can be

thus written as (also see [12]):

$$(4) \quad H_{mayo}(s) = \frac{1}{s + c_1} \frac{1}{s + c_2} \frac{1}{L} (H_{mayo,abs}(s) - 1)$$

The values c_1 and c_2 can be used to eliminate drift and account for the pilot's ability to correct for low-frequency disturbances [12]. When $c_1 = 0$, the first pole becomes an integrator $1/s$, canceling the zero in the origin resulting from $H_{mayo,abs}(s) - 1$. According to Ref. [12], the second additional pole should be set to a low frequency. In the current study $c_1 = 0$ and $c_2 = 0.2\pi$ ($= 0.1 \text{ Hz}$) is used, which is in accordance with Ref. [11] (p. 7). Note that these values can be optimized, but to do so one needs low-frequency BDFT data, which were not obtained in Mayo's experiment. For the current study the length of the collective was determined to be $L = 0.7 \text{ m}$.

Fig. 1 shows the magnitude and phase of the pilot's BDFT dynamics for the collective control input, obtained using Eq. 4 and the aforementioned parameter values. The asterisks in the figure indicate the frequencies where acceleration disturbances were applied in Mayo's study.

2.4. Discussion on the Mayo model

The pilot's dynamics in Fig. 1 are shown for a much larger frequency range than used by Mayo, as the BDFT dynamics also show interesting features outside the 1-5 Hz frequency range [20]. The frequency range used by Mayo was limited and it is therefore likely that the model's quality will reduce outside this range. Furthermore, note that the differences observed between the ecto- and mesomorphic subjects are only small. This observation, in combination with the fact that the results are based on the average over only three subjects for each somatotype, raises the question whether the observed differences are indeed caused by somatotypical differences and are not due to other causes. Finally, the parameter values found for the Mayo model reflect the BDFT dynamics for only one particular setting of the neuromuscular system, namely the neuromuscular settings used to perform the low-frequency tracking task.

At this point, the main goals of the current study can be made explicit. In the current paper, an enhanced BDFT pilot model for rotorcraft is proposed with equal simplicity as the Mayo model, but with increased accuracy and usability through incorporating recently obtained measurement data [28]. The main intended improvements are the following:

- Increase the model's frequency range
- Incorporate the effect of somatotype (between-subject variability);
- Incorporate the effect of neuromuscular admittance (within-subject variability);

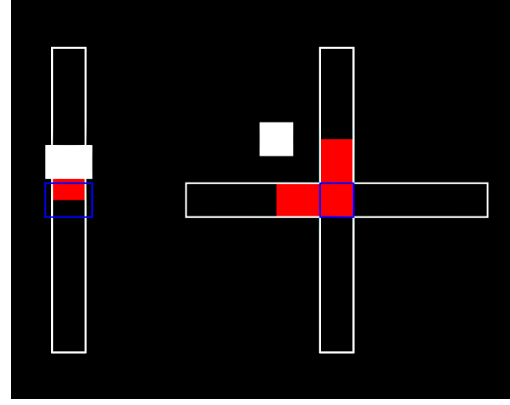


Figure 2: *Display presented to the subject. On the left the collective, on the right the cyclic (roll in horizontal and pitch in vertical direction). The figure shows the collective slightly above target value of 50%. The cyclic is slightly deflected to the left and forward.*

- Compare between- and within-subject variability and determine relative impact

In the following, the adapted Mayo model, Eq. 4, will be used as model structure, for which new parameter values will be identified. To avoid confusion between models, the model obtained in this study will be referred to as the 'BDFT model', or $H_{BDFT}(s)$. This model will be compared to 'Mayo model' with the original ecto- and mesomorphic parameters, $H_{mayo}^{ecto}(s)$ and $H_{mayo}^{meso}(s)$ respectively.

3. METHODS

For the current study, new BDFT data were obtained in an experiment. For a detailed description of this experiment, the reader is referred to Ref. [28]. In the following, the description is summarized.

3.1. Experiment description

3.1.1. Apparatus

The experiment was performed on the SIMONA Research Simulator of Delft University of Technology, a six degree-of-freedom flight simulator. The control devices were electrically actuated collective and cyclic controls with adjustable dynamics settings. The settings used for each control axis were based on [29] and are listed in Table 1. The seat in which the subjects were seated had a 5-point safety belt that was adjusted tightly. Performance information could be displayed on a 15" LCD screen in front of the subject, see Fig. 2.

Table 1: Control device dynamical settings

Axis	Inertia (Ns^2/deg)	Damping (Ns/deg)	Stiffness (N/deg)
Cyclic pitch	0.0369	0.0514	1.8340
Cyclic roll	0.0162	0.0516	1.8100
Collective	0.0152	0.0447	1.7950

Table 2: Data of subjects (N=12).

	Age ($years$)	Weight (kg)	Height (cm)	BMI (kg/m^2)
mean	27.9	75.0	179.9	23.1
stdev	4.3	12.2	6.5	2.8
Range	23-38	58-105	167-190	19.9-29.1

3.1.2. Subjects

Fourteen subjects participated in the experiment. All subjects were right-handed. Before analyzing the data, the results of two subjects were removed, due to insufficient performance. See Table 2 for the subject data of the remaining twelve subjects. The body-mass-index (BMI) utilizes a person's height (in m) and weight (in kg), and is a measure of the total amount of body fat in adults [30]. BMI is calculated by dividing weight by height squared.

3.1.3. Experiment design

During the experiment, two disturbance signals were used simultaneously: an acceleration disturbance $M_{dist}(t)$, applied to the simulator, and a force disturbance $F_{dist}(t)$ applied to the control devices. Using the acceleration disturbance M_{dist} , the BDFT dynamics were determined; force disturbance F_{dist} permitted obtaining the neuromuscular admittance. Motion disturbance M_{dist} consisted of a translational acceleration signal, applied to a single axis of the simulator. Force disturbance F_{dist} consisted of a force signal, applied to a single axis of the control device. The direction of M_{dist} and F_{dist} were always aligned. The measurements were performed for three disturbance directions (DIR): lateral (LAT), longitudinal (LNG) and vertical (VRT).

The subjects were instructed to perform three disturbance rejection tasks (TSK) [31]: position task (PT), in which the instruction is to keep the position of the side-stick in the centered position, that is, to "resist the force perturbations as much as possible"; force task (FT), in which the instruction is to minimize the force applied to the side-stick, that is, to "yield to the force perturbations as much as possible"; relax task (RT), in which the instruction is to relax the arms while holding the control devices, that is, to "passively undergo the perturbations". For the PT the best per-

formance was achieved by being very stiff (low admittance), the FT required the operator to be very compliant (high admittance). The RT yielded an admittance reflecting the passive dynamics of the neuromuscular system. Each task was trained before the experiment started. In earlier studies, it was shown that the neuromuscular admittance and BDFT strongly depend on these control tasks [21, 20]. The three tasks combined with the three directions results in a 3x3 repeated-measures design, each condition was repeated 6 times. During the experiment the angular deflection of the side-stick θ_{CD} and the applied force to the side-stick F_C were measured.

3.1.4. Disturbance signal design

Both disturbance signals, F_{dist} and M_{dist} , were multi-sines, defined in the frequency domain. The signals were separated in frequency to allow distinguishing the response due to each disturbance in the measured signals [31, 20]. The frequency content of the disturbance signals was equal in all conditions, only the magnitude varied for each task. The magnitude was varied in such a way that the standard deviation of the control device deflections was approximately similar in each condition to allow comparison across conditions [20]. To obtain a full bandwidth estimate of the admittance, a range between 0.05 Hz and 21.5 Hz was selected for the force disturbance signal F_{dist} . This frequency range will be referred to as ω_f . For the motion disturbance signal M_{dist} , a range between 0.1 and 21.5 Hz was selected, which will be referred to as ω_m . Note that ω_m is a much larger frequency range than used in Ref. [1], which allows for expanding the model's frequency range. For ω_f 31 logarithmically spaced frequency points were selected in the frequency range, for ω_m 36 frequency points were selected (see Ref. [28] for details). There existed no overlap between ω_f and ω_m .

3.2. Analysis

The biodynamic feedthrough dynamics are calculated using the estimated cross-spectral density between $M_{dist}(t)$ and $\theta_{CD}(t)$ ($\hat{S}_{md,\theta}(j\omega_m)$) and the estimated auto-spectral density of $M_{dist}(t)$ ($\hat{S}_{md,md}(j\omega_m)$):

$$(5) \quad \hat{H}_{BDFT}(j\omega_m) = \frac{\hat{S}_{md,\theta}(j\omega_m)}{\hat{S}_{md,md}(j\omega_m)}.$$

The procedure to calculate $\hat{H}_{BDFT}(j\omega_m)$ assumes linearity. To check the reliability of this assumption

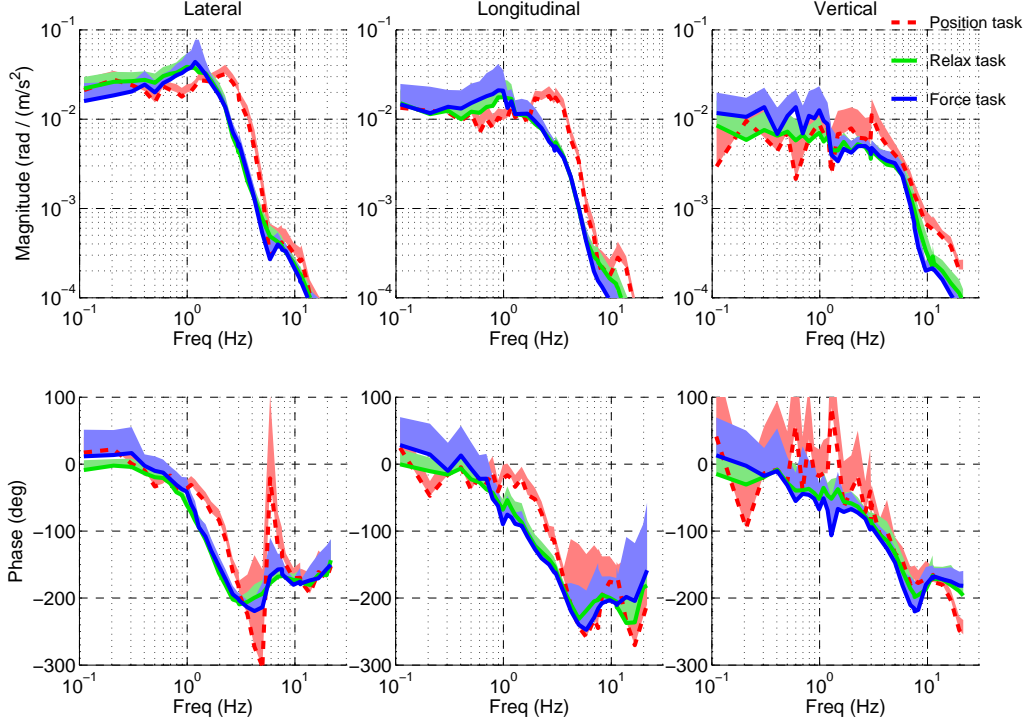


Figure 3: Magnitude and phase of the BDFT dynamics obtained per direction and per task. The results were obtained by averaging over all subjects.

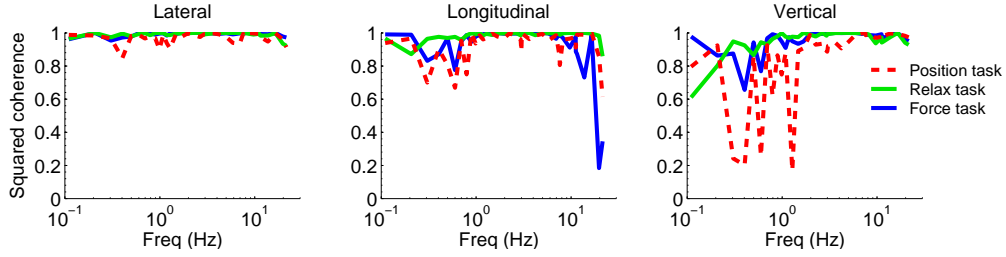


Figure 4: Coherence of the BDFT dynamics obtained per direction and per task. The results were obtained by averaging over all subjects.

the squared coherence was calculated:

$$(6) \quad \hat{\Gamma}_{BDFT}^2(j\omega_m) = \frac{|\hat{S}_{md,\theta}(j\omega_m)|^2}{\hat{S}_{md,md}(j\omega_m)\hat{S}_{\theta,\theta}(j\omega_m)}.$$

The squared coherence is a value between zero and one and a measure of the signal-to-noise ratio (SNR) and thus for the linearity of the dynamic process. This function equals one when neither non-linearities nor time-varying behavior exist [32].

The neuromuscular admittance dynamics was estimated in a similar way to how the BDFT dynamics were obtained, but now using the force disturbance F_{dist} . As the results of the admittance analysis will not be discussed in the current paper, no further details on that analysis will be provided here (see Refs. [28, 20] instead).

3.3. Parameter estimation

The parameters of the BDFT model were estimated by fitting the BDFT model on \hat{H}_{BDFT} . The latter was obtained using Eq. 5 on the measurement data for each subject and then averaging over all subjects, for each control task. The estimation was performed by minimization of the total squared logarithmic difference between the measured and modeled BDFT dynamics, with the following error criterion:

$$(7) \quad E_{B2P} = \sum_{\omega_m} \left| \log \left[\frac{\hat{H}_{BDFT}(\omega_m)}{\bar{H}_{BDFT}(\omega_m)} \right] \right|.$$

\hat{H}_{BDFT} is the Frequency Response Function (FRF) of the biodynamic feedthrough estimate and \bar{H}_{BDFT} is the FRF of the BDFT model.

During the parameter estimation it was observed that

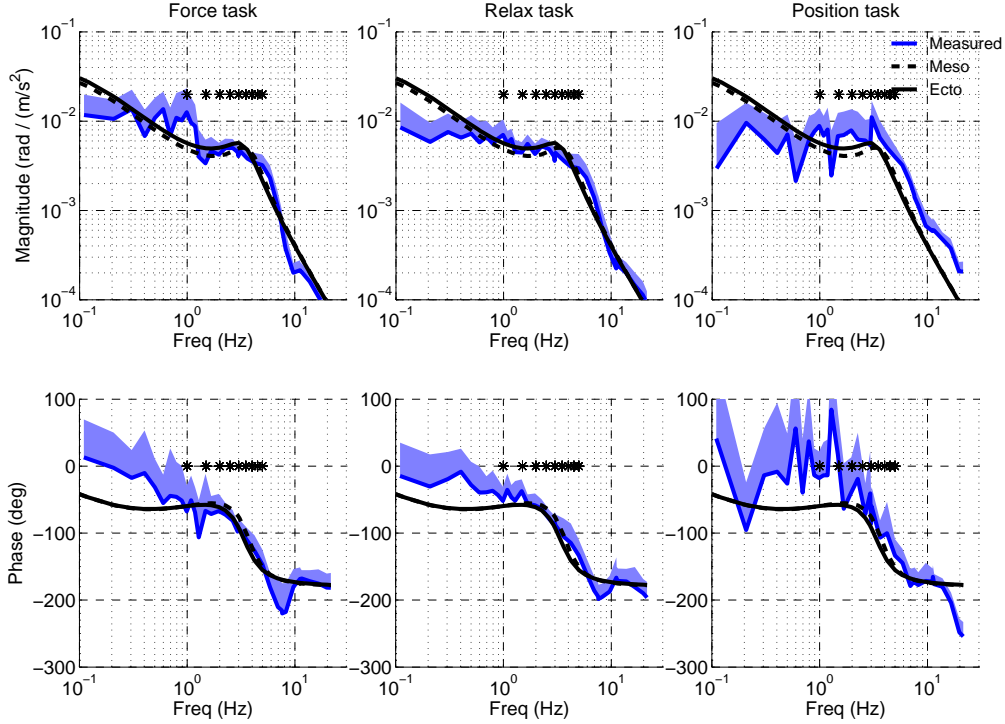


Figure 5: *The Mayo model applied to the measurement data in vertical direction.*

a_1 was estimated to be zero or close to zero in each condition. Therefore, this parameter was fixed to zero, to prevent over-parameterization. This did not lead to an increase in E_{B2P} . Also parameter c_1 was fixed to a value of zero, as was done in Ref. [12] (see Section 2.3). The parameters that remained to be estimated were a_2 , b_1 , and b_2 (from Eq. 1) and c_2 (from Eq. 4).

4. RESULTS

4.1. Non-parametric estimates

Fig. 3 shows the measured pilot BDFT magnitude and phase, averaged over all subjects, for each condition, grouped per disturbance direction. The means over the subjects are indicated by the lines, the standard deviations by the colored bands (mean + 1 standard deviation is shown). It can be observed that the BDFT dynamics depend on both disturbance direction and task. More particularly, it can be observed that for all three directions, for disturbances above 1-2 Hz, the PT results in the highest level of BDFT. For this task, also a peak in the BDFT level can be observed between approximately 2 and 3 Hz for each direction. This implies that 'stiff' behavior, although largely beneficial at lower frequencies, is the worst strategy when dealing with motion disturbances above 1-2 Hz [28]. Note that between-subject variability was largely re-

moved by averaging over all subjects. The differences in BDFT dynamics observed between control tasks can be interpreted as the (averaged) within-subject variability. As these differences are considerable, it can be concluded that within-subject BDFT variability is an important factor that should be accounted for.

The squared coherence obtained for each task and each direction is shown in Fig. 4. The coherences found in the lateral and longitudinal direction are close to 1 for each frequency and task, indicating that reliable estimates were obtained in these directions. For the vertical direction, the squared coherences for the RT and FT are acceptable; for the PT the coherences are considerably lower and therefore the data cannot be assumed to be reliable. The most likely cause of the low coherence is the limited motion space of the SIMONA simulator in the vertical direction [28].

The data obtained from the relax and force task can be considered sufficiently reliable to be used to extend Mayo's model. The analysis of the position task data will be provided in the following as well but the results should be interpreted as exploratory. The analysis of the experimental data in the longitudinal and lateral direction – where good coherences were achieved – is an interesting future extensions of the BDFT pilot model to these axes. However, as Mayo model only refers to the vertical axis, these data are not further analyzed in the current study.

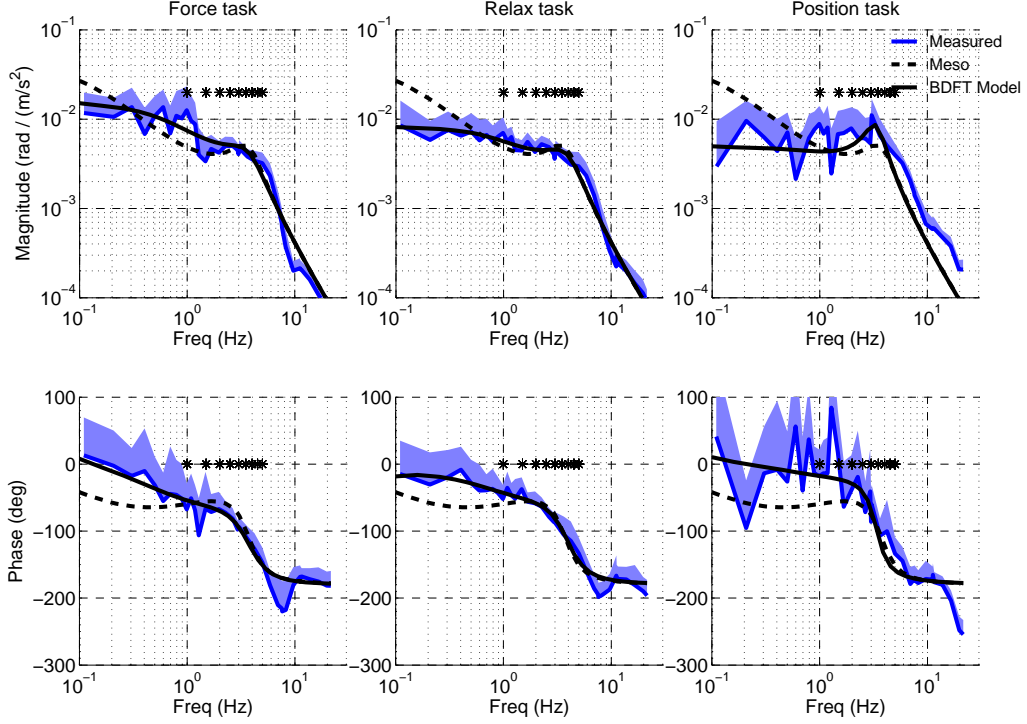


Figure 6: The BDFT model applied to the measurement data in vertical direction.

4.2. Performance of the Mayo model

Fig. 5 shows the Mayo model, for both ecto- and mesomorphic subjects (taken from Fig. 1), superimposed on the BDFT data obtained for the three control tasks in the vertical direction (taken from the right-most column in Fig. 3). Again, the asterisks indicate the locations where Mayo applied sinusoidal motion disturbances. It can be observed that for these frequencies the model fits reasonably well to the data obtained in this study. Especially for the RT the model provides an adequate description. This is what was to be expected, as it is likely that the subjects in Mayo's study performed the control task with moderate admittance, that is, not extremely stiff nor extremely compliant. Note that for the other control tasks the model is less accurate in this frequency range. Outside this frequency range, the performance of the model decreases even further, for all tasks. This shows there is ample room for improvement in the Mayo model.

4.3. Performance of the BDFT model

After estimating the parameters, as described above, the BDFT model for the three control tasks become:

$$(8) \quad H_{BDFT}^{FT}(s) = \frac{1}{0.7s(s+3.26)} \left(\frac{554.00}{s^2 + 18.00s + 550.36} - 1 \right)$$

and
(9)

$$H_{BDFT}^{PT}(s) = \frac{1}{0.7s(s+5.57)} \left(\frac{447.56}{s^2 + 8.28s + 446.42} - 1 \right)$$

and
(10)

$$H_{BDFT}^{RT}(s) = \frac{1}{0.7s(s+5.06)} \left(\frac{597.82}{s^2 + 17.23s + 599.81} - 1 \right)$$

Note that the parameters presented for the position task in Eq. 9 are exploratory only.

Fig. 6 shows the BDFT model, as developed in this paper and with its parameters estimated as described above, superimposed on the BDFT data obtained for the three control tasks in the vertical direction. The (mesomorphic) Mayo model is also shown for comparison. From the plots it becomes clear that the BDFT model describes the measured BDFT dynamics well, both in magnitude and phase. It can also be observed that for each control task the BDFT model dynamics are different, signifying the influence of the neuromuscular dynamics across tasks. When comparing with the Mayo model, it is clear that the BDFT model provides a more accurate description of the measured BDFT dynamics. Note that the model quality for the PT is not as high as for the other tasks. The reason for this is twofold: first, the quality of the data obtained for this task in this direction was rather poor, resulting into a rather noisy BDFT estimate, with peaks and jitter, which cannot – and should not – be

Table 3: Non-zero model parameters ($a_1 = c_1 = 0$)

BDFT Model		a_2	b_1	b_2	c_2
All	FT	554.00	18.00	550.36	3.26
	PT	447.56	8.28	446.42	5.57
	RT	597.82	17.23	599.81	5.06
Ecto	FT	642.62	21.04	639.52	3.31
	PT	572.54	14.01	573.64	5.51
	RT	604.76	24.47	618.51	7.12
Meso	FT	564.27	16.13	561.30	2.81
	PT	418.93	8.02	418.01	6.02
	RT	579.05	16.87	579.56	5.98
Endo	FT	443.50	21.01	437.26	4.55
	PT	458.48	6.23	454.44	4.47
	RT	603.63	15.60	603.63	3.07
Mayo Model		a_2	b_1	b_2	a_1
Ecto	–	452.30	13.70	452.30	5.19
Meso	–	555.40	13.31	555.40	4.02

described by the model. Second, the model structure seems unable to describe the BDFT dynamics at higher frequencies, or more precisely: the model underestimates the BDFT magnitude for frequencies above approx. 4 Hz. This can be solved by adjusting the model structure, which will not be done here. Note that up to 4 Hz the model structure seems to be adequate.

The parameters for the different control task are shown visually in Fig. 7 and numerically in Table 3 in the row labeled 'All (subjects)'. Note that for each task similar values were obtained for parameters a_2 and b_2 . In the Mayo model the same value was used for both parameters (parameter values also shown in Table 3, note that the last column shows a_1). The current results suggest that parameters a_2 and b_2 can be substituted by one parameter without reducing the model quality severely (not done here).

When using these parameter values to model BDFT in other experimental setups, it is important to note that the parameter values are depending on the control device settings used in this study, see Table 1. The validity of the parameter values will decrease when the control device dynamics strongly deviate from the dynamics used in this study. The development of a model for which its parameter values are independent from control device dynamics is currently under investigation.

4.4. Influence of somatotypes

To investigate between-subject variability, subjects were grouped according to BMI. The BMI is recognized as proxy for somatotype [30, 33]. In Ref. [30]

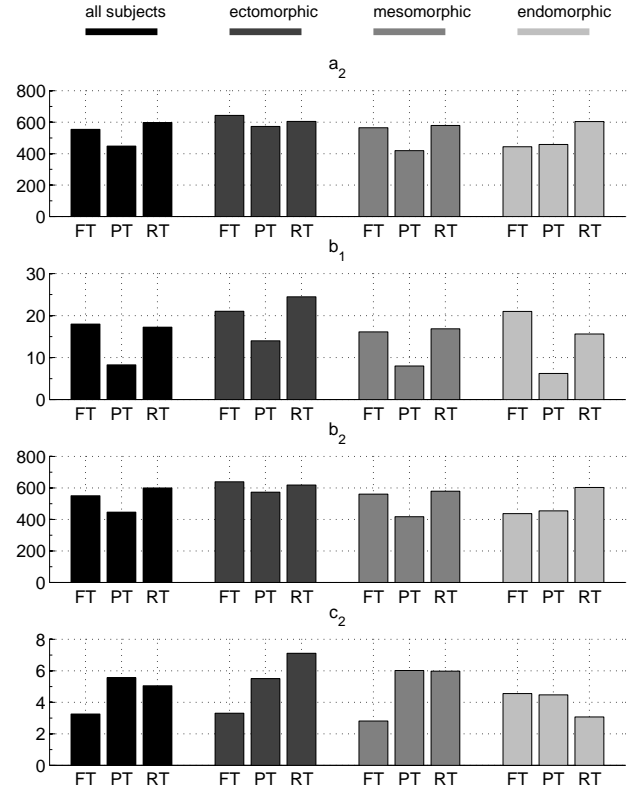


Figure 7: The BDFT model parameters for all subject and the different somatotypes.

it was proposed that a BMI score below 19 can be classified as ectomorph, a BMI score between 19 and 25 as mesomorph and a BMI score above 25 as endomorph. From the 12 subjects that participated in the current study, two were endomorphic according to this classification. The two subjects that were closest to being ectomorphic (with a BMI around 20) were assigned to the ectomorphic group. The remaining eight subjects had a BMI between 20.5 and 25.1 and can be classified as mesomorphic. See Table 4 for the data of the subjects in each group.

Interestingly enough, the subjects that participated in Mayo's study were classified as ectomorphic and mesomorphic. However, based on their average height and weight, their BMIs are 22.5 and 26.1 respectively and, according to Ref. [30], these BMI values would qualify as meso- and endomorphic somatotypes.

Fig. 8 shows the BDFT magnitude averaged for each somatotype group, per control task, superimposed on the BDFT magnitude for 'all subjects' (the grand average BDFT). Before discussing the results, it is important to note that the ectomorphic and endomorphic groups only consist of two subjects, making the data vulnerable to outliers. Also note that for the grand average BDFT only the positive standard deviation is

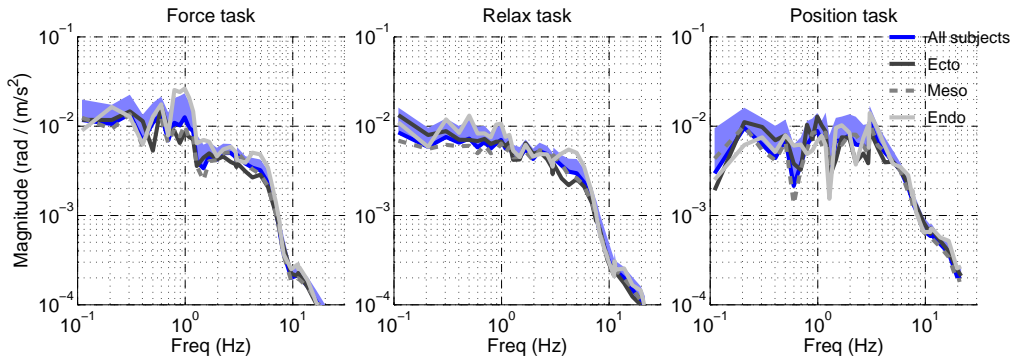


Figure 8: The BDFT dynamics measured for different somatotypes.

indicated. Taking those notions into account, it can be observed that the BDFT data for the somatotypic groups shows only small differences with respect to each other or the grand average BDFT. The variation typically lies within one standard deviation of the grand average. This observation can be interpreted as evidence that the somatotype of the subjects only has a modest influence on the BDFT dynamics. Table 3 and Fig. 7 show the model parameters obtained for each somatotypic groups. Also here it can be said that the differences between control tasks seem larger than between somatotypic groups. Note that the parameters obtained for the mesomorphic group are very similar to those obtained for all subjects, as is to be expected because this somatotypic group contains 8 of the 12 subjects. The differences with and between the ecto- and endomorphic group do not show an obvious structural trend. In the authors' opinion, the results do not allow to conclude that the observed differences are solely due to somatotypic influence on BDFT. In fact, it seems probable that they stem merely from the random variation in the measurement. Recall that also in Mayo's study the differences reported between somatotypes were small. Combining these observations provides reason to question whether categorizing BDFT dynamics according to somatotype is sensible in the first place. Possibly, other sources of variation show a clearer and more significant influence. The model parameters for the three different somatotypes were presented here, however the authors would like to stress that a structural influence of somatotype on BDFT dynamics is absent. From the results it has become apparent, though, that neuromuscular admittance does have a clear influence on BDFT and definitely needs to be accounted for (see also [22]).

5. CONCLUSIONS AND DISCUSSION

In this study, a practical biodynamic feedthrough model was developed, containing seven parameters

Table 4: Data of somatotypical groups

Ectomorphic subjects (N=2)				
	Age (years)	Weight (kg)	Height (cm)	BMI (kg/m ²)
mean	23.5	68.0	184.0	20.07
stdev	0.7	5.7	8.5	0.2
Mesomorphic subjects (N=8)				
	Age (years)	Weight (kg)	Height (cm)	BMI (kg/m ²)
mean	28.3	71.7	177.6	22.67
stdev	4.5	8.0	5.6	1.7
Endomorphic subjects (N=2)				
	Age (years)	Weight (kg)	Height (cm)	BMI (kg/m ²)
mean	31.0	95.0	185.0	27.7
stdev	0.0	14.1	7.1	2.0

(six pilot parameters + one control device parameter). The model's structure was based on a BDFT model proposed by Mayo in Ref. [1] and adapted according to Ref. [12]. Model parameters were estimated using recently obtained BDFT measurement data. The data provide BDFT dynamics in different directions and for different control tasks, each requiring a different neuromuscular setting. In the current paper the data of the vertical direction was used.

Results show that the model describes the measured data well and that it provides a considerable improvement to the original Mayo model. The BDFT dynamics and model parameters differ for each control task, indicating that the neuromuscular setting has an important influence on the BDFT dynamics which needs to be addressed in the BDFT model.

The BDFT dynamics and model parameters were also compared between different somatotypes (body types). Results show that the influence of somatotype on BDFT dynamics is only modest. The authors would like to stress that although an influence of body type is to be expected, the current results do not show a structural effect. Therefore, the authors would advise against differentiating between body types in

BDFT modelling, as long as proof for a structural influence on BDFT dynamics and model parameters is absent.

An important question that needs answering is which set of parameters would be most applicable for a helicopter pilot in ordinary conditions. As the pilot typically controls the helicopter using a rather loose grip and a relaxed muscular setting, the parameters obtained for the relax task seem the most appropriate. This selection is supported by the observation that the Mayo model, obtained during a tracking task, matched largely with the relax task dynamics. One could imagine, however, that in case of an emergency or increased workload the pilot could 'stiffen up', making the position task parameters more appropriate. The authors would like to stress that, in this experiment, the parameters obtained for this task were based on data with low coherences and are therefore exploratory. A neuromuscular setting used during force task is less likely to occur under normal conditions. This setting is typically used when following haptic cues from a haptic controller (providing forces to the control device that the pilot needs to follow); such controllers are not commonly implemented in current helicopters.

In future publications, the model will be extended to the other axes. Moreover, new model structures will be investigated. In this study, the structure proposed by Mayo was used, and although adequate, the results can surely be improved by using a different, higher order, model structure, for example to describe the higher frequency behavior during the position task. Also, the influence of the control device dynamics and control device position on the BDFT dynamics should be investigated. Finally, it would be interesting to test and compare the performance of the models in the time domain. This will allow to compare the models in a more intuitive sense and in addition, such an approach will shed more light on the influence of somatotype on BDFT dynamics.

ACKNOWLEDGEMENTS

Heinrich H. Bülthoff was supported by the myCopter project, funded by the European Commission under the 7th Framework Program.

REFERENCES

[1] J. R. Mayo, "The involuntary participation of a human pilot in a helicopter collective control loop," in *ERF 1989 15th European Rotorcraft Forum, Amsterdam, the Netherlands*, Sep. 1989, pp. 81-001 – 81-012.

- [2] H. Humphreys, W. Book, and J. Huggins, "Compensation for biodynamic feedthrough in backhoe operation by cab vibration control," in *IEEE International Conference on Robotics and Automation (ICRA)*, May 2011, pp. 4284 – 4290.
- [3] D. L. Raney, E. B. Jackson, C. S. Buttrill, and W. M. Adams, "The impact of structural vibrations on flying qualities of a supersonic transport," in *AIAA Atmospheric Flight Mechanics Conference, Montreal, Canada*, Aug. 2001.
- [4] R. A. Hess, "Theory for roll-ratchet phenomenon in high-performance aircraft," *Journal of Guidance, Control and Dynamics*, vol. 21, no. 1, pp. 101–108, 1998.
- [5] D. Banerjee, L. M. Jordan, and M. J. Rosen, "Modeling the effects of inertial reactions on occupants of moving power wheelchairs," in *Rehabilitation Engineering and Assistive Technology Society of North America Conference (RESNA)*, Salt Lake City, UT, USA, Jun. 1996.
- [6] V. V. Rodchenko, L. E. Zaichik, and Y. P. Yashin, "Handling qualities criterion for roll control of highly augmented aircraft," *Journal of Guidance, Control and Dynamics*, vol. 26, no. 6, pp. 928 – 934, Nov. 1993.
- [7] B. P. Lee, V. V. Rodchenko, L. E. Zaichik, and Y. P. Yashin, "Simulation - to - flight correlation," in *AIAA Modeling and Simulation Technologies Conference, Austin, TX, USA*, Aug. 2003.
- [8] R. Gabel and G. J. Wilson, "Test approaches to external sling load instabilities," *Journal of the American Helicopter Society*, vol. 13, no. 3, pp. 44 – 54, 1968.
- [9] R. B. Walden, "A retrospective survey of pilot-structural coupling instabilities in naval rotorcraft," in *American Helicopter Society 63rd Annual Forum, Virginia Beach, VA, USA*, May 2007, pp. 897–914.
- [10] O. Dieterich, J. Götz, B. DangVu, H. Haverdings, P. Masarati, M. D. Pavel, M. Jump, and M. Gennaretti, "Adverse rotorcraft-pilot coupling: Recent research activities in europe," in *ERF 2008 34th European Rotorcraft Forum, Liverpool, United Kingdom*, Sep. 2008.
- [11] P. Masarati, G. Quaranta, M. Gennaretti, and J. Serafini, "Aeroservoelastic analysis of rotorcraft-pilot coupling: a parametric study," in *AHS 2010 American Helicopter Society 66th Annual Forum, Phoenix, AR, USA*, Sep. 2010.

- [12] P. Masarati, G. Quaranta, and M. Jump, "Experimental and numerical helicopter pilot characterization for aeroelastic rotorcraft-pilot couplings analysis," *Proceedings of the Institution of Mechanical Engineers, Part G: Journal of Aerospace Engineering*, Dec. 2011.
- [13] G. Quaranta, P. Masarati, and J. Venrooij, "Robust stability analysis: a tool to assess the impact of biodynamic feedthrough on rotorcraft," in *AHS 2012 American Helicopter Society 68th Annual Forum, Forth Worth, TX, USA*, May 2012.
- [14] P. Masarati, G. Quaranta, L. L., and M. Jump, "Theoretical and experimental investigation of aeroelastic rotorcraft-pilot coupling," in *AHS 2012 American Helicopter Society 68th Annual Forum, Forth Worth, TX, USA*, May 2012.
- [15] M. D. Pavel, J. Malecki, B. DangVu, P. Masarati, M. Gennaretti, M. Jump, M. Jones, H. Smaili, A. Ionita, and L. Zaicek, "Present and future trends in rotorcraft pilot couplings (rpcs): A retrospective survey of recent research activities within the european project ARISTOTEL," in *ERF 2011 37th European Rotorcraft Forum, Gallarate, Italy*, Sep. 2011, pp. 275 – 293.
- [16] M. D. Pavel, "A retrospective survey of adverse rotorcraft pilot couplings in european perspective," in *AHS 2012 American Helicopter Society 68th Annual Forum, Forth Worth, TX, USA*, May 2012.
- [17] R. W. McLeod and M. J. Griffin, "Review of the effects of translational whole-body vibration on continuous manual control performance," *Journal of Sound and Vibration*, vol. 133, no. 1, pp. 55 – 115, 1989.
- [18] S. Sövényi and R. B. Gillespie, "Cancellation of biodynamic feedthrough in vehicle control tasks," *IEEE Transactions on Control Systems Technology*, vol. 15, no. 6, pp. 1018 – 1029, Nov. 2007.
- [19] J. Venrooij, M. Mulder, M. M. van Paassen, D. A. Abbink, and M. Mulder, "A review of biodynamic feedthrough mitigation techniques," in *11th IFAC/IFIP/IFORS/IEA Symposium on Analysis, Design, and Evaluation of Human-Machine Systems, Valenciennes, France*, Sep. 2010.
- [20] J. Venrooij, D. A. Abbink, M. Mulder, M. M. van Paassen, and M. Mulder, "A method to measure the relationship between biodynamic feedthrough and neuromuscular admittance," *IEEE Transactions on Systems, Man, and Cybernetics, Part B: Cybernetics*, vol. 41, no. 4, pp. 1158 – 1169, 2011.
- [21] —, "Biodynamic feedthrough is task dependent," in *SMC 2010 IEEE International Conference on Systems, Man and Cybernetics, Istanbul, Turkey*, Oct. 2010, pp. 2571 – 2578.
- [22] J. Venrooij, M. Mulder, M. M. van Paassen, D. A. Abbink, H. H. Bülthoff, and M. Mulder, "Cancelling biodynamic feedthrough requires a subject and task dependent approach," in *SMC 2011 IEEE International Conference on Systems, Man, and Cybernetics, Anchorage, AK, USA*, Oct. 2011, pp. 1670 – 1675.
- [23] H. R. Jex and R. E. Magdaleno, "Biomechanical models for vibration feedthrough to hands and head for a semisuspine pilot," *Aviation, Space, and Environmental Medicine*, vol. 49, no. 1, pp. 304 – 316, 1978.
- [24] P. Masarati, G. Quaranta, J. Serafini, and M. Gennaretti, "Numerical investigation of aeroservoelastic rotorcraft-pilot coupling," in *AIDAA 2008 XIX Congresso Nazionale AIDAA, Forlì, Italy*, Sep. 2007.
- [25] M. Mataboni, A. Fumagalli, M. Jump, P. Masarati, and G. Quaranta, "Biomechanical pilot properties identification by inverse kinematics/inverse dynamics multibody analysis," in *ICAS 2008, 26th Congress of the International Council of the Aeronautical Sciences, Anchorage, AK, USA*, Sep. 2008.
- [26] J. Serafini, M. Gennaretti, P. Masarati, G. Quaranta, and O. Dieterich, "Aeroelastic and biodynamic modeling for stability analysis of rotorcraft-pilot coupling phenomena," in *ERF 2008 34th European Rotorcraft Forum, Liverpool, United Kingdom*, Sep. 2008.
- [27] W. Sheldon, S. S. Stevens, and W. B. Tucker, *The varieties of human physique: An introduction to constitutional psychology*. Harper and Brothers Publishers, 1940.
- [28] J. Venrooij, D. Yilmaz, M. D. Pavel, G. Quaranta, M. Jump, and M. Mulder, "Measuring biodynamic feedthrough in helicopters," in *ERF 2011 37th European Rotorcraft Forum, Gallarate, Italy*, Sep. 2011, pp. 967 – 976.
- [29] D. Mitchell, R. Hoh, A. J. Adolph, and D. Key, "Ground based simulation evaluation of the effects of time delays and motion on rotorcraft handling qualities," Tech. Rep. USAAVSCOM TR 91-A-010, AD-A256 921, Jan. 1992.
- [30] S. Maddan, J. T. Walker, and J. M. Miller, "Does size really matter? a reexamination of sheldon's somatotypes and criminal behavior," *The Social Science Journal*, vol. 45, pp. 330 – 344, 2008.

- [31] D. A. Abbink, "Neuromuscular analysis of haptic gas pedal feedback during car following," Ph.D. dissertation, Delft University of Technology, 2006.
- [32] F. C. T. van der Helm, A. C. Schouten, E. de Vlugt, and G. G. Brouwn, "Identification of intrinsic and reflexive components of human arm dynamics during postural control," *Journal of Neuroscience Methods*, vol. 119, no. 1, pp. 1–14, 2002.
- [33] S. Maddan, J. T. Walker, and J. M. Miller, "The BMI as a somatotypic measure of physique: a rejoinder to Jeremy E.C. Genovese," *The Social Science Journal*, vol. 46, pp. 394 – 401, 2009.